Article

Discovery Medicine 2024; 36(183): 799–815
https://doi.org/10.24976/Discov.Med.202436183.75

Herbo-Mineral Medicine, Lithom Exhibits Anti-Nephrolithiasis Activity in Rat Model of Hyperoxaluria by Attenuating Calcium Oxalate Crystal Formation and Oxidative Stress

Acharya Balkrishna[1,2,3], Sandeep Sinha[1], Moumita Manik[1], Anupam Pandey[1], Madhulina Maity[1], Rishabh Dev[1], Anurag Varshney[1,2,4,*]

[1]Drug Discovery and Development Division, Patanjali Research Foundation, 249405 Haridwar, Uttarakhand, India
[2]Department of Allied and Applied Sciences, University of Patanjali, 249405 Haridwar, Uttarakhand, India
[3]Patanjali Yog Peeth (UK) Trust, G41 1AU Glasgow, UK
[4]Special Centre for Systems Medicine, Jawaharlal Nehru University, 110067 New Delhi, India
*Correspondence: anurag@patanjali.res.in (Anurag Varshney)
Published: 20 April 2024

Background: Calcium oxalate monohydrate (COM) forms the most common type of kidney stones observed in clinics, elevated levels of urinary oxalate being the principal risk factor for such an etiology. The objective of the present study was to evaluate the anti-nephrolithiatic effect of herbo-mineral formulation, Lithom.

Methods: The *in vitro* biochemical synthesis of COM crystals in the presence of Lithom was performed and observations were made by microscopy and Scanning Electron Microscope (SEM) based analysis for the detection of crystal size and morphology. The phytochemical composition of Lithom was evaluated by Ultra-High-Performance Liquid Chromatography (UHPLC). The *in vivo* model of Ethylene glycol-induced hyperoxaluria in Sprague-Dawley rats was used for the evaluation of Lithom. The animals were randomly allocated to 5 different groups namely Normal control, Disease control (ethylene glycol (EG), 0.75%, 28 days), Allopurinol (50 mg/kg, *q.d.*), Lithom (43 mg/kg, *b.i.d.*), and Lithom (129 mg/kg, *b.i.d.*). Analysis of crystalluria, oxalate, and citrate levels, oxidative stress parameters (malondialdehyde (MDA), catalase, myeloperoxidase (MPO)), and histopathology by hematoxylin and eosin (H&E) and Von Kossa staining was performed for evaluation of Lithom.

Results: The presence of Lithom during COM crystals synthesis significantly reduced the average crystal area, feret's diameter, and area-perimeter ratio, in a dose-dependent manner. SEM analysis revealed that COM crystals synthesized in the presence of 100 and 300 µg/mL of Lithom exhibited a veritable morphological transition from irregular polygons with sharp edges to smoothened smaller cuboid polygons. UHPLC analysis of Lithom revealed the presence of Trigonelline, Bergenin, Xanthosine, Adenosine, Bohoervinone B, Vanillic acid, and Ellagic acid as key phytoconstituents. In EG-induced SD rats, the Lithom-treated group showed a decrease in elevated urinary oxalate levels, oxidative stress, and renal inflammation. Von Kossa staining of kidney tissue also exhibited a marked reduction in crystal depositions in Lithom-treated groups.

Conclusion: Taken together, Lithom could be a potential clinical-therapeutic alternative for management of nephrolithiasis.

Keywords: Lithom; ethylene glycol; oxalate; nephrolithiasis; anti-oxidant; anti-inflammatory

Introduction

Nephrolithiasis also known as 'kidney stones' or 'renal calculi' is estimated to be one of the most prevalent diseases that affects 1 in 11 individuals, with a recurrence rate of 50% within 10 years of first detection [1]. The recurrence rate of the disease remains elevated even after surgical interventions. The symptoms of nephrolithiasis include painful urination, hematuria with sharp abdominal pain, or a characteristic loin to groin pain. It is the third most commonly occurring urinary disorder with an average male to female occurrence ratio of 2:1 [2–4]. Nephrolithiasis is a gradual process where calcium ions/oxalates/phosphates of calcium start to accumulate in distal tubules and collecting ducts of nephrons [5]. In renal calculi, supersaturation of ions may aggravate as a consequence of multiple factors like inadequacy of inhibitors such as citric acid or abundance of promoters such as oxalate-rich diet or lack of hydration. These factors increase the level of urinary ions to concentrations beyond their normal dissolution rates [2,6]. Over time, nucleation initiates followed by aggregation and eventual crystal growth which causes depositions, injury, and associated pain. The formation of small-sized crystals is often non-symptomatic and they are easily flushed through urine, whereas larger calculi cause obstruction and injuries to nephrons and to urinary tract. The interaction of

calcium oxalate monohydrate (COM) crystals has been observed with cultured renal tubular cells, where the expression of some receptors facilitates crystal adhesion, growth, and depositions [7].

Kidney cells could also internalize crystals on exposure, resulting in either crystal dissolution or transcytosis through the epithelial layer. This modulates normal cellular functions like mitogenesis and activation of specific signaling pathways. Additional outcomes include membrane lysis, cell necrosis or apoptosis and production of reactive oxygen species. The interaction of various types of crystals with primary inner medullary collecting duct cells demonstrates saturability and inhibition to a certain degree of one crystal type by others. Renal calculi are composed of calcium oxalate, calcium phosphate, uric acid, and magnesium phosphates [1]. Other than these certain drugs also induce calculus formation. Calcium oxalate crystals are the most common types. They exist in two forms, sharp and polygonal-shaped calcium oxalate monohydrate (COM) and blunt calcium oxalate dihydrate (COD). COM has sharp edges that facilitate its adhesion with renal epithelial cells rendering them more harmful than COD [8]. COM is thermodynamically more stable than COD due to a solid apatite core which attracts the smaller crystals facilitating conglomeration. Whereas COD crystals are less porous and have a low supersaturation rate, hence COM transition into COD paves the way for its expulsion by urine [9]. The current treatments for nephrolithiasis include oral administration of diuretics, which facilitates the elimination of crystals through frequent micturition [10,11]. Whereas the large-sized crystals either need invasive surgery called percutaneous nephrolithotomy (PCNL) for their removal or a non-invasive technique known as extracorporeal shock wave lithotripsy (ESWL) where high energy shock waves are given from outside the body to break the crystal into pieces to facilitate their expulsion [12]. None of these techniques are helpful when it comes to the recurrence of nephrolithiasis [13]. Moreover, oral administration of diuretics in excess can lead to adverse effects like hypokalemia, hyperglycemia, and glucose intolerance [14,15]. Therefore, interventions having no adverse effects and which offer diminution of large crystals with subsequent prevention of their formation would be worthwhile alternatives to current treatment options for nephrolithiasis.

Traditional herbal formulations have been widely used for various remedial purposes since ages. Several preclinical studies describe the therapeutic potential of herbal formulations in ailments pertaining to vital organs like kidney [16] and liver [17]. As per classical Ayurvedic scriptures like Sharangadhara samhita, the active compounds in polyherbal formulation have much more therapeutic efficacy than the individual plant itself, when combined in a fixed ratio [18]. Ayurvedic medicinal science is the most ancient yet living system of medicine, being able to tackle deficiencies of the contemporary system, like adverse effects of drugs, lack of curative treatment for several chronic conditions, and cost of expensive drugs. Almost 60% of the global population has renewed interest in herbal medicines [19,20]. Lithom is a polyherbal formulation prepared with components like puncture vine (*Tribulus terrestris*), red hogweed (*Boerhavia diffusa*), horse gram (*Doliochus biflorus*), fenugreek (*Trigonella foenum graecum*), winter begonia (*Saxifraga ligulata*), three leaved capers (*Crataeva nurvula*). Each of these herbs has proven anti-urolithiatic properties, in several *in vitro* and *in vivo* studies [21–26]. Some classical Ayurvedic formulations are also included in the preparation of Lithom as enlisted in Table 1. In the present study, we investigated the inhibitory effect of Lithom on COM crystallization using *in vitro* cell-free assays and *in vivo* model of ethylene glycol-induced nephrolithiasis in rats. Allopurinol was used as a concurrent method control in this study. Additionally, a detailed phytochemical analysis of Lithom was conducted on the Ultra-High-Performance Liquid Chromatography (UHPLC) platform, to assign the observed biological effects with the active phytocompounds present in the formulation.

Materials and Methods

Reagents

Lithom tablets (Internal batch number D4/CHM/SARA-014/119) were sourced from Divya Pharmacy, Haridwar, India. Standards and solvents used for UHPLC based quantification of Lithom: Trigonelline (Cat# T002, Potency 90%, Natural remedies, Bangalore, Karnataka, India), Adenosine (Cat# A9251, Potency-99.9%, Sigma-Aldrich, Saint Louis, MO, USA), Xanthosine (Cat# X0008, Potency-99.6%, TCI, Chennai, Tamil Nadu, India), Bergenine (Cat# B4349, Potency-99.7%, TCI, Chennai, Tamil Nadu, India), Vanillic acid (Cat# 68654, Potency-98.2%, Sigma-Aldrich, Saint Louis, MO, USA), Boeravinone B (Cat# B011, Potency-97.0%, Natural remedies, Bangalore, Karnataka, India) and Ellagic acid (Cat# E2250, Potency-99.6%, Sigma-Aldrich, Saint Louis, MO, USA), acetonitrile (Cat# 40030LC250, Finar, Ahmedabad, Gujarat, India), methanol (Cat# M0276, Rankem, Gurugram, Haryana, India), and acetic acid AR grade (Cat# A0070, Rankem, Gurugram, Haryana, India). Ethylene glycol (EG, Cat# E0105) was purchased from TCI, Chennai, Tamil Nadu, India. Ammonium chloride (Cat# 25103) and calcium chloride dihydrate were purchased from SRL Pvt. Ltd, Mumbai, Maharashtra, India. Allopurinol tablets of a standard brand (Zyloric, GSK, Mumbai, Maharashtra, India) were procured from the local vendor. Methylcellulose (high viscosity) 4000 CPS (Cat# 04635) was procured from Loba Chemie, Mumbai, Maharashtra, India. The standard pellet diet (18% Protein-5L79) purchased from Purina LabDiet, Saint Louis, MO, USA. Sodium oxalate was obtained from Rankem, Gurugram, Haryana, India. Animal bedding

Table 1. Composition of Lithom.

S.No.	Constituents	Common name	Plant parts	Weight
1	*Tribulus terrestris*	Puncture vine	Fruit	50 mg
2	*Dolichos biflorus*	Horse gram	Seed	50 mg
3	*Crataeva nurvula*	Three leaved caper	Bark	50 mg
4	*Boerrhavia diffusa*	Red Hogweed	Root	20 mg
5	*Saxifraga ligulata*	Winter Begonia	Root	20 mg
6	*Trigonella foenum graecum*	Fenugreek	Seed	10 mg
7	*Yava khsara*	Classical Ayurvedic preparation	-	100 mg
8	*Hazrul yahud bhasma*	Classical Ayurvedic preparation	-	50 mg
9	*Kalmi shora*	Classical Ayurvedic preparation	-	20 mg
10	*Mulaka khsara*	Classical Ayurvedic preparation	-	80 mg
11	*Swet parpati*	Classical Ayurvedic preparation	-	50 mg

material, Sparcobb was purchased from Sparconn Life Sciences, Bangalore, Karnataka, India. All other chemicals used in the study were purchased from Sigma-Aldrich, Saint Louis, MO, USA.

In vitro Synthesis of Calcium Oxalate Monohydrate (COM) Crystals

COM crystals were synthesized as per the methods described by Chaiyarit *et al*. [27]. 10 mM calcium chloride dihydrate ($CaCl_2H_4O_2$) and 1 mM sodium oxalate ($Na_2C_2O_4$) solutions were prepared in 10 mM Tris-HCl and 90 mM NaCl, pH adjusted to 7.5. Lithom dilutions (2 µg/mL–200 µg/mL, 2×) were prepared in 1 mM $Na_2C_2O_4$ solutions. In a 24-well plate, 10 mM $CaCl_2H_4O_2$ and Lithom dilution (2×) in 1 mM $Na_2C_2O_4$ were mixed in 1:1 (v/v) ratio and were allowed to shake slowly at room temperature for 1 hour. Analysis of formed crystals in the presence and absence of Lithom was carried out using Zeiss PrimoVert (Carl Zeiss India, Bangalore, Karnataka, India). More than 100 crystals were chosen from five different fields (×200 magnification) for each experimental condition.

Scanning Electron Microscope (SEM) Based Analysis of Synthesized COM Crystals

COM crystals were synthesized on coverslips. After 1 hr, reaction solutions were removed and coverslips were allowed to dry at room temperature. Samples were monitored through a scanning electron microscope (FlexSEM1000, Hitachi, Chiyoda-ku, Tokyo, Japan) and visualized at 5kV using SEM MAP software (ver. 01-10, Hitachi, Chiyoda-ku, Tokyo, Japan).

UHPLC Method

UHPLC samples were prepared by diluting 1 gm powdered Lithom tablets with 10 mL methanol and water (80:20) and sonicated for 30 min, followed by centrifugation at 10,000 rpm for 5 min. The solution was filtered by a 0.45 µm nylon filter and utilized for the analysis. Sample analysis was performed by Prominence-XR UHPLC system (Shimadzu, Kyoto, Japan) equipped with a Quaternary pump (Nexera XR LC-20AD XR), DAD detector (SPD-M20 A), Auto-sampler (Nexera XR SIL-20 AC XR), Degassing unit (DGU-20A 5R) and Column oven (CTO-10 AS VP). Chromatographic separation was achieved using a Shodex-4E C18 (5 µm, 4.6 × 250 mm) column subjected to binary gradient elution. The two solvents used for the analysis were 0.1% acetic acid in water (solvent A) and acetonitrile (solvent B). Gradient programming of the solvent system was initially at 100% A from 0–10 min, 100–95% A from 10–25 min, 95–92% A from 25–30 min, 92–75% A from 30–45 min, 75–30% A from 45–60 min, 30–100% A from 60–61 min, 100% A from 61–70 min, with a flow rate of 1.0 mL/min. 10 µL of standard and test solution were injected and column temperature was maintained at 35 °C. Wavelengths were set at 270 nm for Trigonelline, Xanthosine, Bergenin, Vanillic acid, Boeravinone B; and 250 nm for Ellagic acid and Adenosine. The compounds were identified and quantified by comparison with the standard mix using Shimadzu Labsolutions software (ver. 6.89, Shimadzu, Kyoto, Japan).

Experimental Animals

Six to eight weeks old healthy Specific-Pathogen-Free (SPF) male Sprague-Dawley rats, weighing between 150–200 g, were procured from Hylasco Biotechnology (India) Pvt. Ltd, Mumbai, Maharashtra, India, a Charles River Laboratory licensed experimental animal supplier. The animal husbandry practices and experimental procedures were conducted in conformance with the guidelines from the Committee for the Purpose of Control and Supervision of Experiments on Animals (CPCSEA) Government of India. Before the commencement of the study, the experimental procedures were duly approved by the Institutional Animal Ethics Committee of Patanjali Research Foundation, Haridwar (vide protocol # PRIAS/LAF/IAEC-082). Post procurement, animals were quarantined for a period of one week, before shifting to the experimental room dedicated to the study. Both the quarantine room and the experimental room are located in a registered experimental animal facility

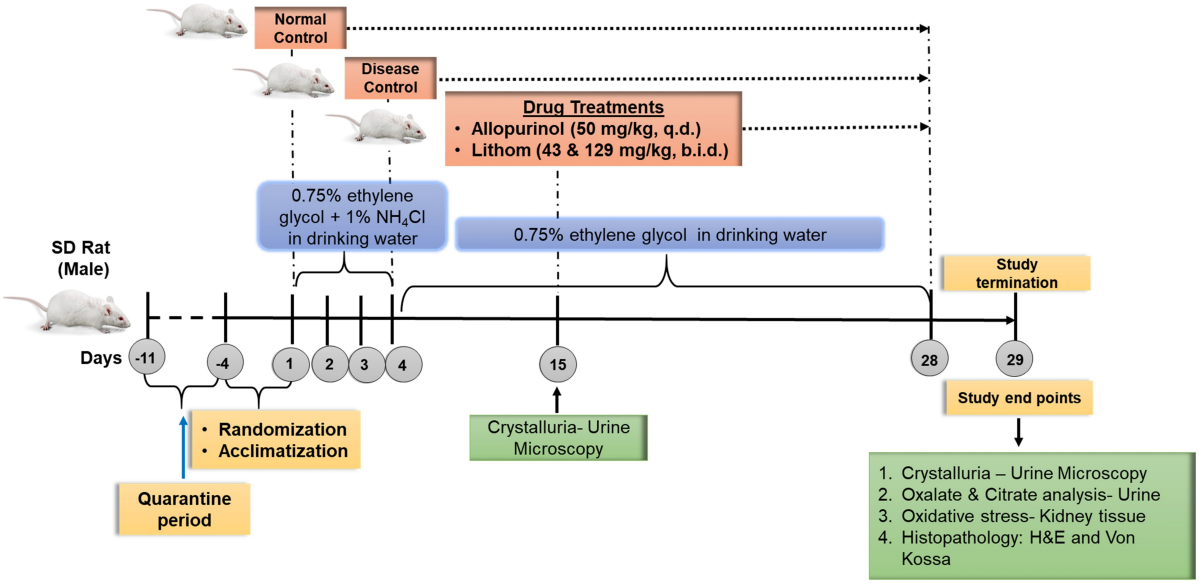

Fig. 1. Experimental design for *in vivo* study. Schematic illustrates the entire study plan providing the details of the experimental groups and their administered doses. The animals were quarantined up to 1 week before their grouping. The animals were randomly allocated to 5 different groups namely Normal control, Disease control, Allopurinol (50 mg/kg, *q.d.*), Lithom (43 mg/kg, *b.i.d.*), and Lithom (129 mg/kg, *b.i.d.*). The normal control group received normal drinking water, whereas the remaining four groups were administered 0.75% ethylene glycol-supplemented drinking water for 28 consecutive days, to induce nephrolithiasis. Two weeks post-induction of nephrolithiasis, animals were treated by oral gavage with either the vehicle, Allopurinol 50 mg/kg, *q.d.* or Lithom at the doses of 43 mg/kg and 129 mg/kg, *b.i.d.*, respectively. Urine samples from rats were collected to analyze crystalluria, oxalate, and citrate levels. Rats were sacrificed at the end of the experiment, kidneys were harvested and used for the analysis of oxidative stress parameters (Catalase, malondialdehyde (MDA), myeloperoxidase (MPO)), and histological assessment of pathology. This figure was prepared in Microsoft Office Powerpoint 2016.

(CPCSEA registration # 1964/PO/Rc/S/17/CPCSEA). The rats were housed under 12 h light-dark cycle. Temperature and relative humidity in the experimental animal room were maintained between 23 ± 2 °C and 30–70% respectively. Animals were offered a standard nutritionally stable pellet diet and sterile drinking water *ad libitum*. Animals were sacrificed by intraperitoneal injection of thiopental sodium (#LU173B/3, Thiosol sodium, Neon Laboratories, Mumbai, Maharashtra, India) at the dose of 150 mg/kg.

Dose Calculation for in vivo Experiments

The animal equivalent doses of Lithom for rat studies were estimated based on the body surface area of the animals. The human recommended dose of the Lithom tablet is ~2500 mg/day. Animal equivalent doses (mg/kg) for rats were calculated by multiplying the human equivalent dose (41.66 mg/kg/day) by a factor of 6.2 [28]. Resultant therapeutic equivalent doses for rats were found to be 258 mg/kg/day or 129 mg/kg *b.i.d.* Therefore, 129 mg/kg *b.i.d.* has been taken as therapeutic dose (TD) for rats and one-third value of TD, which is 43 mg/kg *b.i.d.* is taken as low dose (LD) for pharmacological studies.

Experimental Design for in vivo Study

Animals were allocated randomly into 5 groups consisting of 7 animals per group. G1 served as Normal control (NC), and G2 served as Disease control (DC). Animals allocated NC and DC were treated with 0.5% Methylcellulose (MC, vehicle control). Animals of group G3 received a reference compound, Allopurinol 50 mg/kg, *p.o. q.d.*×14D. G4 received Lithom at a dose of 43 mg/kg, *p.o, b.i.d.*×14D, and G5 received Lithom at a dose of 129 mg/kg; *p.o. b.i.d.*×14D. Nephrolithiasis was induced by the administration of 0.75% ethylene glycol (EG) along with 1% ammonium chloride (NH_4Cl) supplemented drinking water in the rats for 3 days. 0.75% EG-supplemented drinking water was further given to animals for a total duration of 28 days. The water bottles supplemented with NH_4Cl and/or EG were replaced every alternate day [29]. An aqueous suspension of the test compound and reference control were formulated by employing 0.5% MC. Vehicle/Test substance (Lithom)/Reference compound (Allopurinol) administration was initiated from day 15 after the confirmation of the development of crystalluria (on day 15) and continued till day 28. The study was terminated by day 29. A schematic of the study design has been mentioned in Fig. 1.

Urine Collection and Crystalluria Estimation

Twenty-four-hour urine samples were collected on day 29 by placing the animals in metabolic cages. 20 µL of 20% sodium azide was used as a preservative. The samples were centrifuged at 2000 ×g for 10 min for the removal of debris. Following urine collection, crystalluria was estimated. The samples were then acidified with a drop of concentrated hydrochloric acid (HCl) and stored at –20 °C for biochemical analysis [30]. Urine samples were spread over a clean glass slide and placed under a light microscope to examine calcium oxalate (CaOX) crystals. The number of urinary crystals per high-power field was counted from ten random fields (×400 magnification) [29].

Urine Citrate Estimation

Urine citrate was estimated by the method reported by Millan *et al*. [31]. For analysis, samples were maintained at room temperature followed by the addition of sodium hydroxide (25%) and 0.2 mol/L magnesium chloride solution and vortexed. The mixture was centrifuged at 4000 ×g for 10 min to obtain phosphate-free urine and supernatant was transferred to sterilized centrifuge tubes and vortexed again. The pH of the supernatant was maintained at 2 with 10 mol/L HCl. To this solution, $FeCl_3$ (18 mmol/L) was added, mixed well and the absorbance was read at 390 nm on an EnVision multimode plate reader (PerkinElmer, Shelton, CT, USA). Citrate at concentrations 0.312, 0.625, 1.25, 2.5, and 5.0 mmol/L were prepared in deionized water and used as standard reference.

Urine Oxalate Estimation

The method described by Bergerman *et al*. [32] was followed for oxalate estimation in urine samples. The samples were mixed with 1 N sulphuric acid followed by the addition of indole reagent along the walls of the tube and mixed properly, which were then heated at 90 °C for 45 min. The samples were cooled and their absorbance was measured at 525 nm on an EnVision multimode plate reader (PerkinElmer, Shelton, CT, USA). The standard curve was generated using oxalate at a concentration ranging from 0.5–3.5 mg/mL.

Excision of Kidney for Biochemical and Histopathological Analysis

Animals were humanely sacrificed using anesthesia on day 29. Both the kidneys were excised carefully and were weighed. The right kidney was fixed in 10% neutral buffer formalin for histopathological analysis, whereas, the left kidney was stored at –80 °C until processed for biochemical analysis [33].

Protein Estimation

Protein estimation in samples was carried out using Pierce BCA protein assay kit (23225, Thermo Scientific, Waltham, MA, USA). Briefly, different concentrations of the BSA were prepared by serial dilutions. 25 µL of each standard and unknown sample was added per well in a 96 well-plate. To each well 200 µL of the BCA reagent was added and mixed by slight shaking. The plate was then incubated at 37 °C for 30 min and absorbance was measured at 562 nm on an EnVision plate reader (MLD2104-0020A, PerkinElmer, Shelton, CT, USA).

Catalase (CAT) Estimation

CAT activity assay was accomplished by using spectrophotometric determination of hydrogen peroxide (H_2O_2) developing a stable composite with Ammonium molybdate. For the assay 50 µL of serum was mixed with 1 mL substrate (65 µmol/mL H_2O_2 in 60 mmol/L phosphate buffer) and pH was adjusted to 7.4 and incubated at 37 °C for 1 min. The enzymatic reaction was stopped by the addition of 1.0 mL of 32.4 mmol/L ammonium molybdate [$(NH_4)_6$ $Mo_7O_{24}.4H_2O$] and the yellow complex of molybdate and hydrogen peroxide (H_2O_2) was measured at 405 nm against reagent blank using EnVision plate reader (MLD2104-0020A, PerkinElmer, Shelton, CT, USA). One-unit CAT decomposes 1 µM of H_2O_2/min under assay conditions. CAT activity was expressed as U/mg protein [34].

MDA Estimation

Malondialdehyde (MDA) estimation was performed following the method described by Heath *et al*. [35]. For the standard curve, different concentrations of the purified MDA ranging from 0.5–7.5 µM were prepared. For the assay, the standards and samples were mixed with thiobarbituric acid in a 2mL centrifuge tube and heated at 96 °C, at thermomixer for 1 hour. The reaction mixture was cooled and centrifuged. Supernatant from the mixture was separated and absorbance was observed at the wavelength of 535 nm on the EnVision plate reader (PerkinElmer, Shelton, CT, USA). MDA level was expressed as nmol/mg protein.

Myeloperoxidase (MPO) Estimation

MPO activity was measured through reaction with 3,3′,5,5′-Tetramethylbenzidine as described by Kettle *et al*. [36]. Briefly, different concentrations of purified MPO standards ranging from 0.4–8.4 µg/mL were prepared to generate a standard curve. 10 µL each of standards and sample were added per well in a 96-well plate, followed by the addition of 80 µL of 0.75 mM H_2O_2 and 110 µL TMB solution (2.9 mM TMB in 14.5% DMSO and 150 mM sodium phosphate buffer adjusted to pH 5.4) and incubated at 37 °C for 5 min. The reaction was stopped by adding 50 µL of 2M H_2SO_4 and absorbance was measured at 450 nm for estimating MPO activity. MPO activity was expressed as U/mg protein.

Table 2. Crystal scoring and inflammation scoring method in kidney.

Crystal Scoring							
Crystal Score:	0 No crystal	1 Few crystals	2 Moderate number of crystals	3 Frequent crystals	4 Abundant crystals	5 Very abundant crystals	6 Closely packed crystals
Description: Number of crystals	0	1–9	10–24	25–49	50–99	100–199	200-More
Inflammation Scoring							
Inflammation Score: (% of tissue involved)	0 None	1 Minimal	2 Mild	3 Moderate	4 Mark	5 Severe	
Description: Tubular Degeneration/Necrosis/ Desquamation, Congestion	0	1–20%	21–40%	41–60%	61–80%	81–100%	

Histopathological Analysis

The kidneys harvested from the euthanized animals were fixed in 10% buffered neutral formalin, embedded in paraffin wax, sliced in solid sections of 3 to 5 µm thickness, and stained with hematoxylin and eosin (H&E) for evaluating the number of oxalate crystals and inflammation associated with it. At the same time, von kossa stain has been used for the evaluation of the deposited crystals. For estimating crystal score, the number of crystals per high-powered field was counted at ten random fields (×400 magnification) and graded using the methods described by Yang *et al*. [37] in a way as mentioned in Table 2 (Upper panel). The inflammation score was estimated on the basis of the percentage of tissue involved in degeneration, desquamation, and congestion as mentioned in Table 2 (Lower panel). Furthermore, the total lesion score was evaluated as a combination of interstitial inflammation, crystal depositions, tubular degeneration, necrosis, desquamation, and congestion. The score of these parameters was assigned as no inflammation, minimal, mild, moderate, mark, and severe when the lesions are involved 0%, 1–20%, 21–40%, 41–60%, and 61–80% of the respective sample section. Images of the histological slides were captured at low (×100) and high (×400) magnification using the Nikon E100 (Eclipse) microscope (Nikon India, Gurugram, Haryana, India) and processed by GT 5.0 image analysis software (GT Vision, Wickhambrook, Suffolk, UK) [37,38]. Images for von kossa stained sections (×100 magnification) were analyzed using Fiji software (v.153t, NIH, Bethesda, MD, USA).

Statistical Analysis

All values are expressed as mean ± Standard Error of Mean (S.E.M) and were analyzed using one-way analysis of variance (ANOVA) followed by Dunnett's method for post hoc analysis. All the statistical analyses were performed on GraphPad Prism version 8 for Windows, GraphPad Software, Boston, Massachusetts, USA, and $p < 0.05$ was considered statistically significant.

Results

Lithom Retarded COM Crystal Synthesis in vitro

In vitro synthesis of COM crystals was carried out as shown in Fig. 2A. Lithom samples have shown efficacy in reducing the size of COM crystals in a dose-dependent manner as shown in (Fig. 2B Upper panel). Microscopic analysis of the synthesized crystals was carried out as mentioned in the materials and method section. The control group consists of large polygonal crystals possessing sharp edges. Lithom at 1 µg/mL and 3 µg/mL concentrations has an effect on the diminution of crystal size and at a concentration of 10 µg/mL has shown its effect on the morphological structure of COM crystals as well. The crystals of the 10 µg/mL group have blunted and circular edges in comparison to the untreated group. As the Lithom dose increased to 30 µg/mL and 100 µg/mL, a significant ($p < 0.0001$) decrease in the size of crystals was observed (Fig. 2B lower panel). To understand the transitions in the morphology of COM crystals with varying doses SEM analysis of the same has been performed where the changes are clearly distinguished, as the crystals having sharp edges in the untreated group (Fig. 3A) from the smooth spherical structured crystals in 100 µg/mL (Fig. 3A) and 300 µg/mL of Lithom groups (Fig. 3A). The regular and spherical shape of the crystals depicts the morphology of COD crystals which is evident by reduced feret's diameter and their area-perimeter ratio. These parameters were significantly ($p < 0.001$) decreased with Lithom treatment in a dose-dependent manner (Fig. 3B,C). The observations from Lithom-treated groups were found to be remarkable and led us to explore its key phytometabolites using UHPLC analysis.

UHPLC-Based Profiling of Lithom Revealed the Presence of Biologically Active Phytometabolites

To identify the phytometabolites present in Lithom, which might be responsible for its beneficial effects, Ultrahigh-Performance Liquid-Chromatography (UHPLC) analysis was carried out. The peaks in the UHPLC

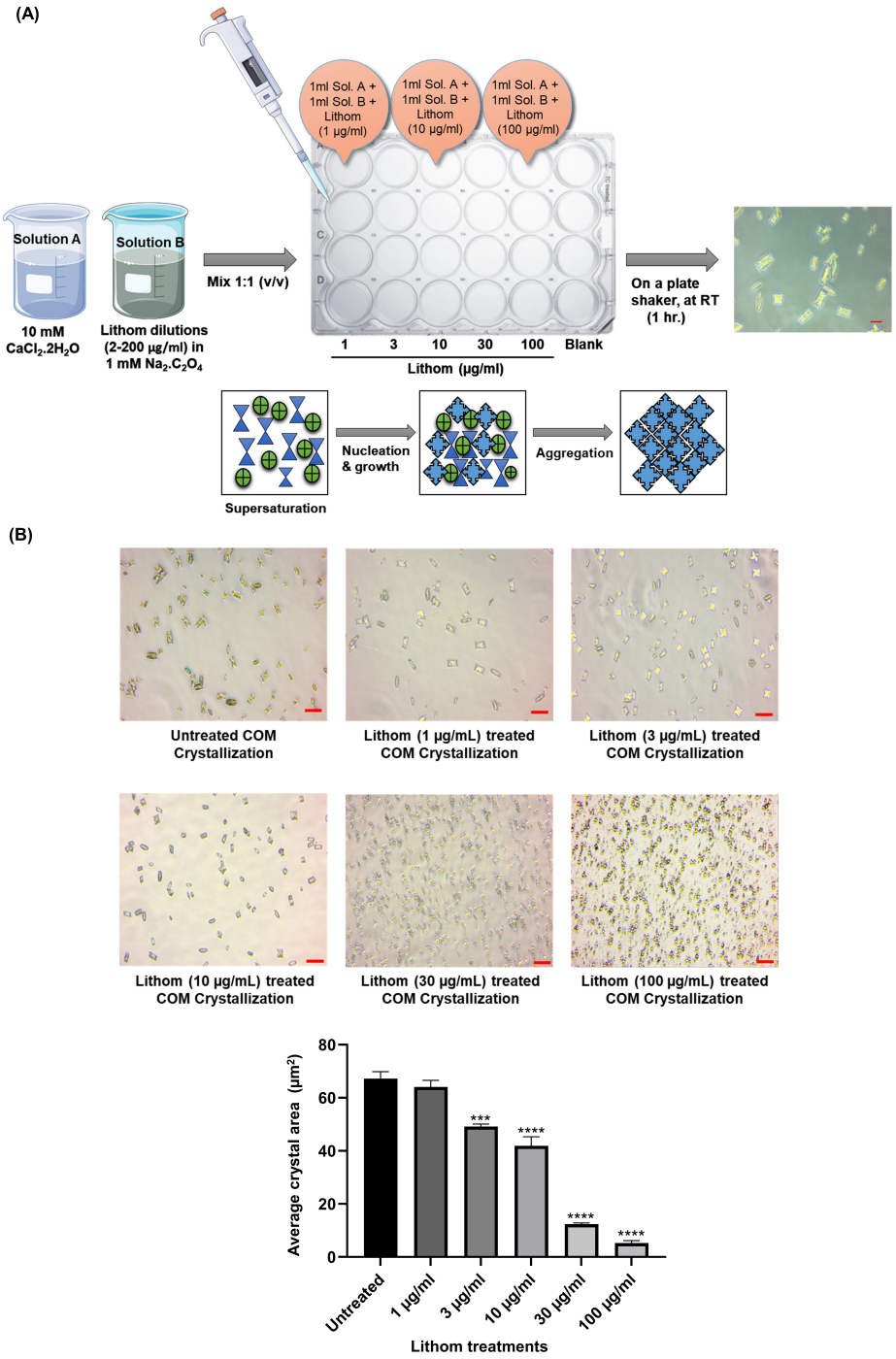

Fig. 2. Effect of Lithom treatment on *in vitro* COM crystallization. (A) Schematic diagram illustrating the process of calcium oxalate monohydrate (COM) crystal formation in presence of Lithom (1–100 µg/mL) (Scale bar = 20 µm). (B) Representative microscopy of COM crystals synthesized in presence and absence of Lithom within 1 hour (Upper panel) (Magnification ×200, Scale bar = 20 µm); Semi-quantitative analysis of COM crystal area using Fiji, showing the efficacy of Lithom in reducing the potential of crystal formation in a dose-dependent manner *in vitro* (Lower panel). Data is presented as mean ± Standard Error of Mean (S.E.M) (n = 3). Statistical significance of the observed difference between the groups was determined through one-way ANOVA and denoted as *** for $p < 0.001$ and **** for $p < 0.0001$ when compared to the untreated group.

chromatogram of Lithom were identified and quantified by direct comparison with known concentrations of standard compounds (Fig. 4). It revealed the presence of Trigonelline 795.67 µg/gm at 3.28 min, Adenosine 93.89 µg/gm at 25.36 min, Xanthosine 2733.26 µg/g at 27.03 min, Bergenin 1803.17 µg/gm at 38.12 min, Vanillic acid 52.66

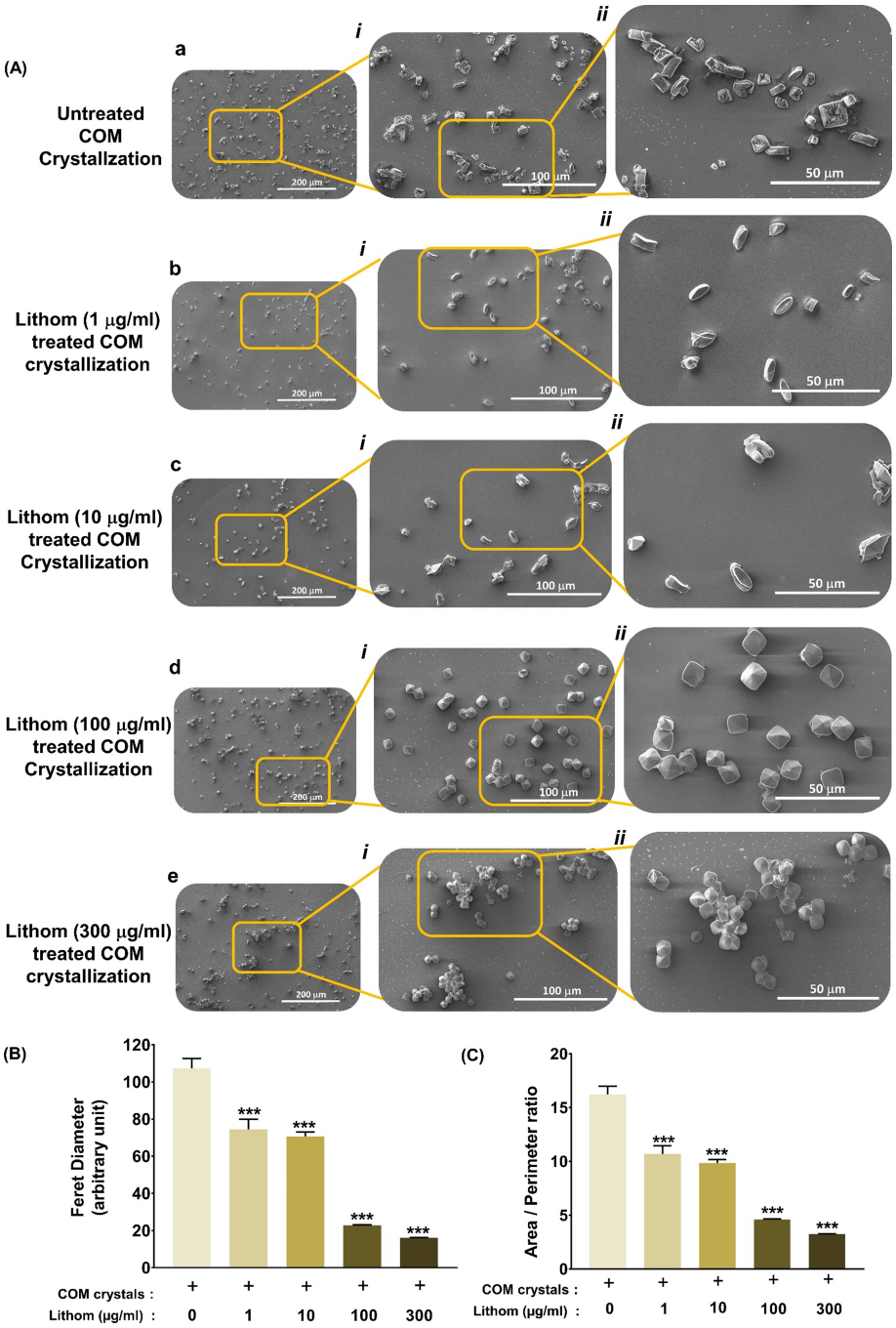

Fig. 3. Scanning Electron Microscope (SEM) analysis for Lithom-mediated transitions in the crystal morphology. (A) Representative SEM images of COM crystals formed in the absence (a) and presence of 1 (b), 10 (c), 100 (d), and 300 µg/mL (e) of Lithom at ×200 magnification. Series of images marked (*i*) and (*ii*), corresponding to each set of the above-mentioned incubation, depict representative fields captured at ×500 and ×1000 magnifications, respectively. (B,C) Quantitative analysis of the SEM images shown in (A) to depict the effect of Lithom treatments on Feret diameters (B) and area-perimeter ratios (C) of COM crystals in each group. Digitally zoomed areas of images at different magnifications were used for the precision of boundary measurement of the crystals. For untreated and 1 µg/mL Lithom treated groups, images at ×1000 magnification were used for quantitative analysis. Images captured at ×500 magnification for 10 µg/mL, and those at ×200 were used for analysis in 100 and 300 µg/mL groups to avoid clusters for accurate measurements of individual crystals. Data is presented as mean ± S.E.M (n = 3). Statistical significance of the observed difference between the groups was determined through one-way analysis of variance (ANOVA) and denoted as *** for $p < 0.001$ when compared to the untreated group.

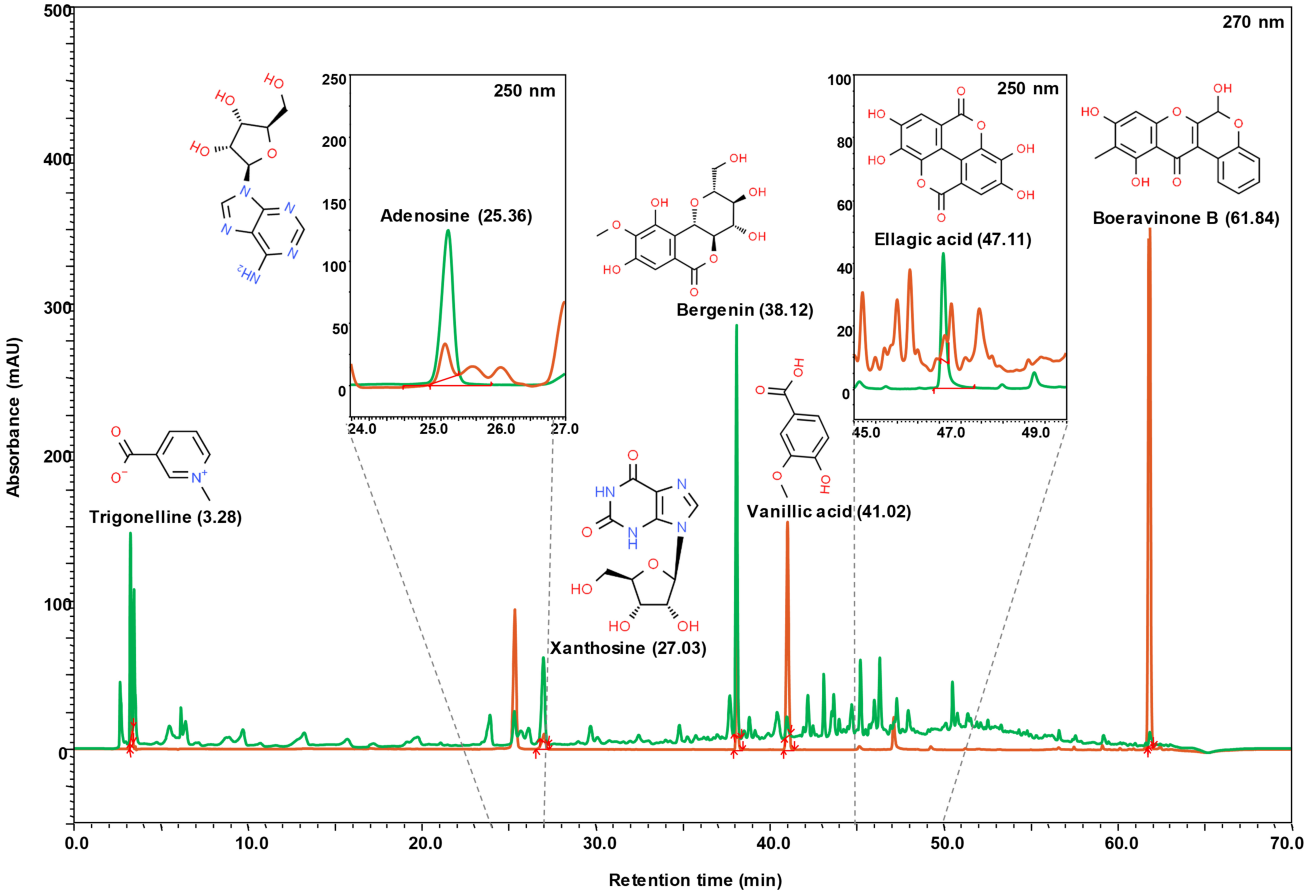

Fig. 4. Quantitative analysis of phytoconstituents of Lithom using UHPLC. Hydromethanolic extract of the Lithom was analyzed to identify the key phytoconstituents present. Seven metabolites were detected at different retention times (RT: min) Trigonelline (RT: 3.28 min), Adenosine (RT: 25.36 min), Xanthosine (RT: 27.03 min), Bergenin (RT: 38.12 min), Vanillic acid (RT: 41.02 min), and Ellagic acid (RT: 47.11 min), Boeravinone B (RT: 61.84 min) at the developed Ultra-High-Performance Liquid Chromatography (UHPLC).

µg/gm at 41.02 min, Ellagic acid 84.02 µg/gm at 47.11 min, Boeravinone B 5.35 µg/gm at 61.84 min of retention times of UHPLC run, as listed in Table 3.

Table 3. Marker compounds obtained from UHPLC analysis of Lithom.

S.No.	Marker compounds	Result (µg/gm)
1	Trigonelline	795.67
2	Adenosine	93.89
3	Xanthosine	2773.26
4	Bergenin	1803.17
5	Vanillic acid	52.66
6	Ellagic acid	84.02
7	Boeravinone B	5.35

Lithom Inhibited EG-Induced Crystalluria in Rats

Crystal formation in experimental rats was induced with 0.75% EG for 28 days. Crystalluria is a condition resulting from the supersaturation of the urine with different ions. EG administration to the rats for 28 consecutive days led to the appearance of COM crystals in urine when compared to normal control group (Fig. 5A). Oral administration of Lithom at the doses of 43 and 129 mg/kg, *b.i.d.* significantly ($p < 0.05$) inhibited EG-induced crystalluria in a dose-related manner (Fig. 5B). Reference control, Allopurinol also showed inhibition in EG-induced crystalluria, at the dose of 50 mg/kg *q.d.* (Fig. 5B, $p < 0.01$).

Lithom Restored Altered Oxalate and Citrate Levels in the Urine of EG-Administered Rats

As determined biochemically, EG administration led to an elevation in the levels of oxalate in the urine, when compared to the normal control group (Fig. 6A). Conversely, the urinary levels of citrate, which acts as the inhibitor of calcium oxalate formation was found to be significantly ($p < 0.05$) lowered (Fig. 6B). Lithom administered groups, at the doses of 43 mg/kg and 129 mg/kg *b.i.d.*, respectively, exhibited significantly ($p < 0.05$) lower oxalate levels, when compared to the disease control group (Fig. 6A). The reference control, Allopurinol also showed effects in diminution of the elevated oxalate

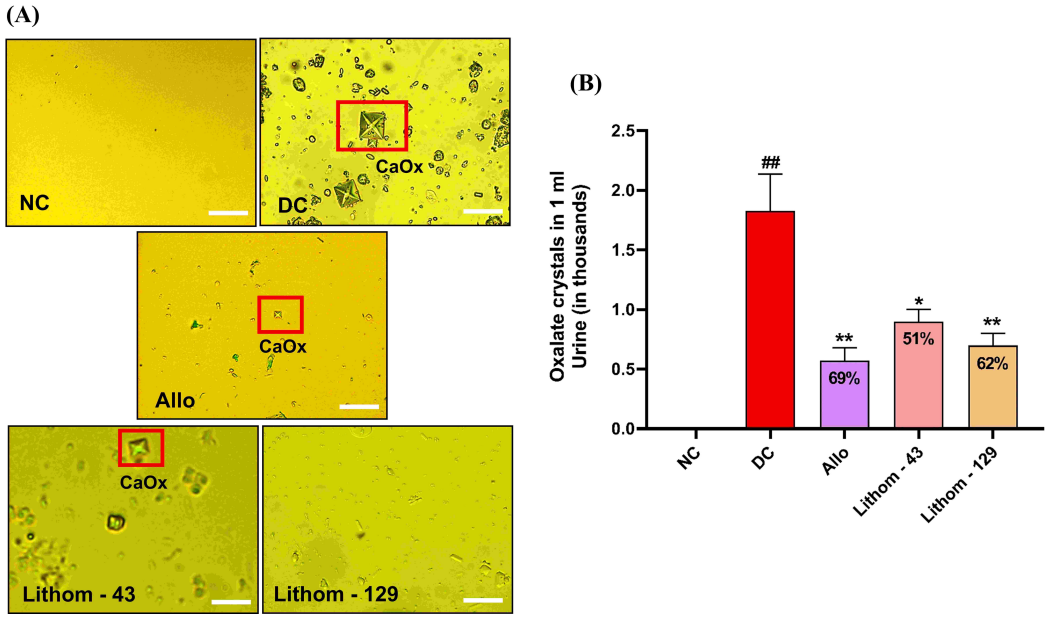

Fig. 5. Microscopic evaluation of crystalluria. (A) Representative images of urine microscopy obtained from the ethylene glycol treated SD Rats with treatments. (B) Quantitative analysis of oxalate crystals per mL of urine. NC represents the normal control group, DC represents the disease control group treated with 0.75% ethylene glycol + 1% NH_4Cl, Allo represents the group treated with standard compound allopurinol 50 mg/kg, *q.d*, Lithom-43 and Lithom-129 represent the groups treated with 43 mg/kg and 129 mg/kg of Lithom, *b.i.d.* respectively. Data is presented as mean ± S.E.M (n = 7 animals per group) and was analyzed by one-way ANOVA followed by Dunnett's multi-comparison test. ## $p < 0.01$ *vs.* NC; * $p < 0.05$; ** $p < 0.01$ *vs.* DC. Scale bar = 100 µm.

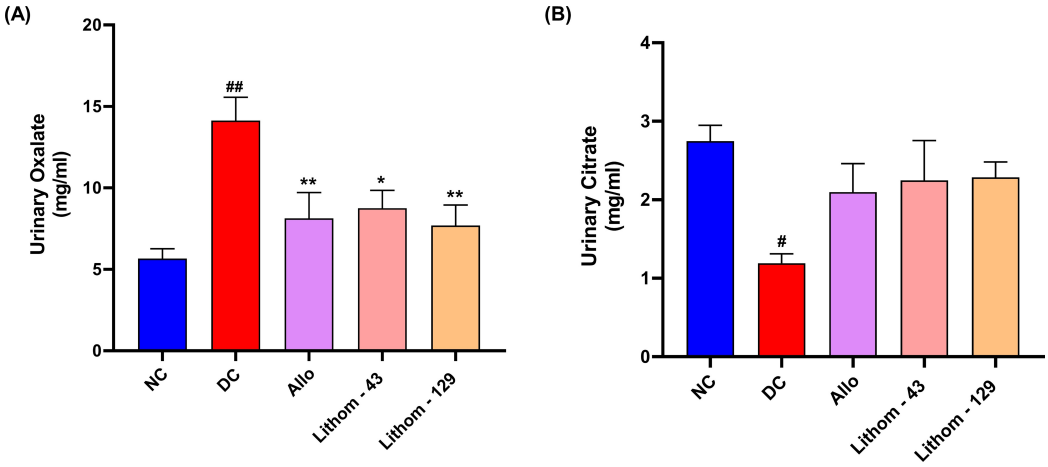

Fig. 6. Evaluation of urine parameters. Quantitative analysis of (A) urinary oxalate level. (B) Urinary citrate level post treatment and represented in mg/mL. Data is presented as mean ± S.E.M (n = 7 animals per group) and was analyzed by one-way ANOVA followed by Dunnett's multi-comparison test. # $p < 0.05$; ## $p < 0.01$ *vs.* NC; * $p < 0.05$; ** $p < 0.01$ *vs.* DC.

levels (Fig. 6A). Further, both Lithom as well as Allopurinol exhibited a trend towards the restoration of urinary citrate levels when compared to the disease-control group (Fig. 6B).

Lithom Ameliorated Crystal-Induced Oxidative Stress in the Kidney

In the nephrolithiatic state, oxidative stress gets elevated in the kidney, as a consequence of crystal-cell interaction leading to Reactive oxygen species (ROS) generation, causing a subsequent imbalance in antioxidant levels in the kidney. Catalase is one of the main antioxidants that balances oxidative stress by conversion of hydrogen peroxide into water. As depicted in Fig. 7A, EG-administration has led to a significant decrease in catalase activity, when compared to the normal control group. Oral administration of Lithom at doses of 43 and 129 mg/kg *b.i.d.* restored catalase activity in rats dose-dependently (Fig. 7A). Allopurinol was not able to exhibit a significant effect on Cata-

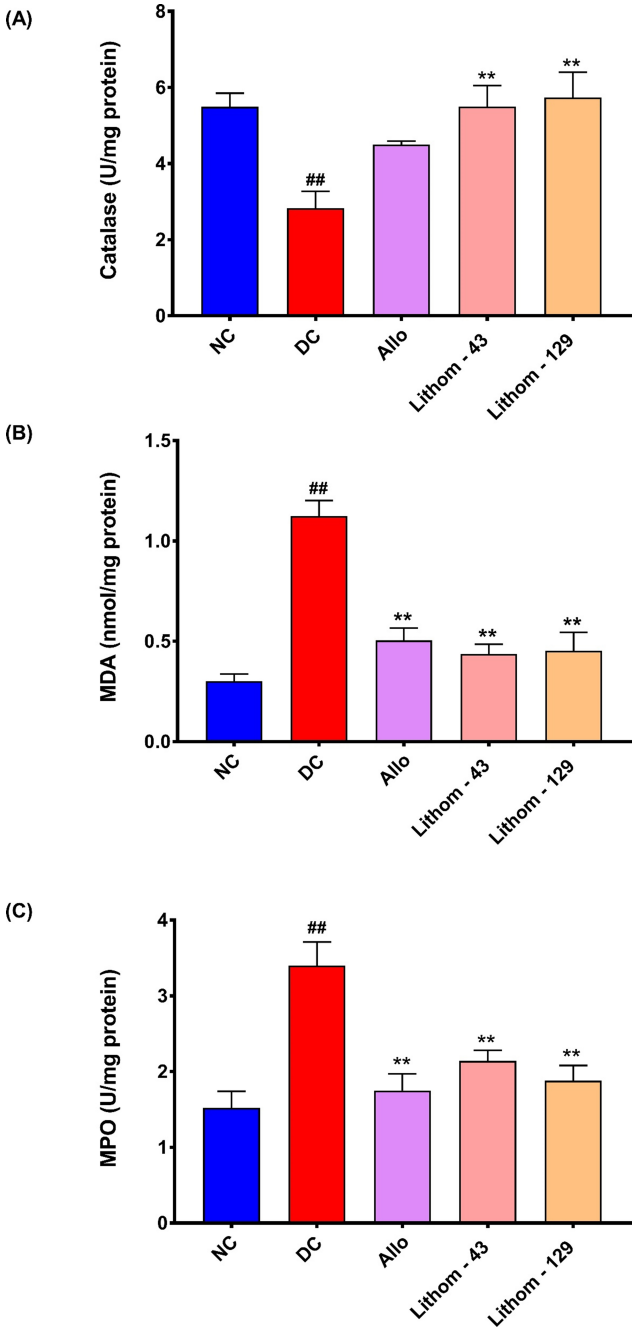

Fig. 7. Evaluation of oxidative stress in the kidney. Quantitative analysis of altered oxidative parameters in the kidney namely (A) Catalase activity; (B) MDA levels; (C) MPO activity and represented as per mg protein. Data is presented as mean ± S.E.M (n = 7 animals per group) and was analyzed by one-way ANOVA followed by Dunnett's multi-comparison test. ## $p < 0.01$ *vs.* NC; ** $p < 0.01$ *vs.* DC.

lase activity (Fig. 7A). Further, malondialdehyde (MDA), which is a marker of oxidative stress and lipid peroxidation was estimated in kidney homogenate. As demonstrated in Fig. 7B, MDA levels were significantly ($p < 0.01$) elevated in the kidneys of animals allocated to the disease control group as compared to a normal control group (Fig. 7B). In the nephrolithiatic state, the rate of lipid peroxidation gets excessively higher, which elevates MDA level. Lithom, administered by oral route at doses of 43 and 129 mg/kg, *b.i.d.* restored elevated MDA levels to near normal values (Fig. 7B). The reference control Allopurinol administered orally at a dose of 50 mg/kg, *q.d.* has also decreased EG-induced elevated MDA levels (Fig. 7B).

The activity of myeloperoxidase (MPO), which catalyzes the generation of several reactive oxygen species has also significantly ($p < 0.01$) elevated in the disease control group, compared to the normal control group (Fig. 7C). Lithom, at both tested doses significantly ($p < 0.01$) decreased the elevated MPO levels in a dose-related manner (Fig. 7C). A similar effect was elicited by Allopurinol at a dose of 50 mg/kg, *p.o.* (Fig. 7C).

Lithom Imparted Renoprotection Against Crystal Induced Injury and Inflammation

The representative histological sections of the normal control group exhibited normal renal parenchyma and no crystal deposition in tubular areas as depicted in Fig. 8A The section represented in the disease control group has shown crystal depositions in proximal convoluted tubule (PCT) and inflammatory changes in surrounding areas, leading to tubular degeneration, necrosis, desquamation, and congestion (Fig. 8A) and hence has elicited a moderate degree of inflammation associated changes in kidneys, when compared to the normal control group (Fig. 8A). Lithom administered by oral route reduced the deposition of crystals in a dose-dependent manner (Fig. 8B). Furthermore, it also reduced associated renal injury and inflammation (In) and promoted the influx of regenerative cells (R) to the surrounding area. Allopurinol also reduced crystal deposition in the kidney and tended to reduce inflammatory changes. To estimate the number of crystals deposited, the degree of inflammation, and the total lesions that occurred of crystal deposition, a scoring criterion was employed as elaborated in the materials and methods section. The crystal and inflammation scores (Fig. 8B,C respectively) were represented separately as well as in combined form as total lesions score in Fig. 8D. Frequent crystals were encountered in the disease control group as compared to the normal control group. Oral administration of Lithom at doses of 43 mg/kg and 129 mg/kg, *b.i.d.* reduced crystal deposition dose-dependently, when compared to the disease control group, and a statistically significant ($p < 0.05$) effect has been observed at 129 mg/kg, *b.i.d.* Allopurinol at 50 mg/kg *b.i.d.* also reduced significantly ($p < 0.05$) the tubular deposition of crystals.

Lithom Prevented Crystal Depositions in the Kidney

For the further analysis of crystal deposition, the von kossa stain has been employed. This particularly stains the calcium crystals black as shown in (Fig. 9 Upper panel). The disease control group exhibited maximum crystal de-

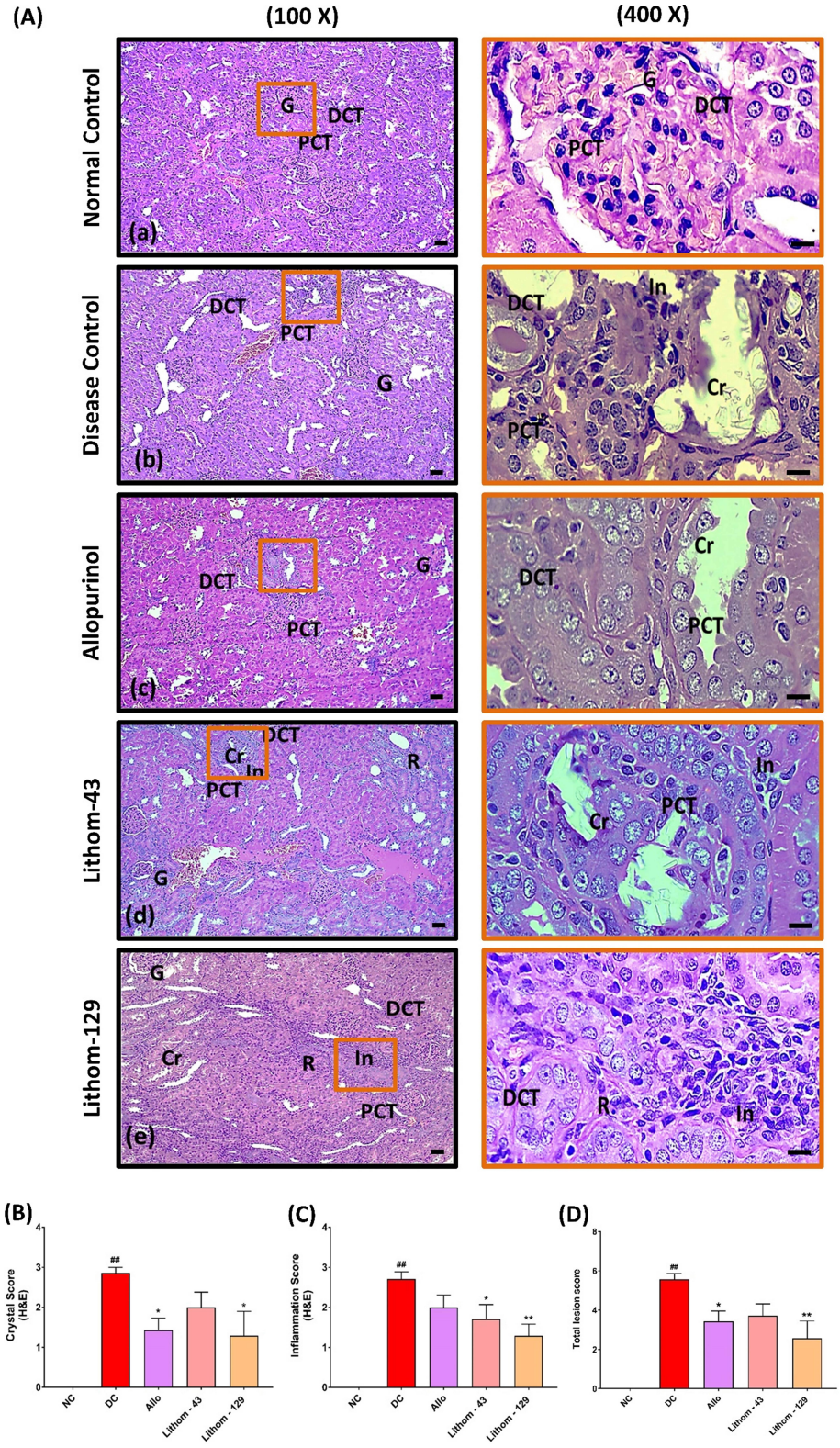

Fig. 8. Hematoxylin and eosin (H&E) staining of kidney sections. (A) Representative images of histopathological sections of kidney stained with H&E. (a) Normal control with no appearance of crystals; (b) Disease control with a high number of crystals at PCT region; (c) Group treated with Allopurinol at 50 mg/kg *q.d*; (d) Lithom at 43 mg/kg *b.i.d* and (e) Lithom at 129 mg/kg b.i.d shows a dose-dependent effect in prevention of crystal retention. (B) Crystal score. (C) Inflammation score. (D) Total lesion score. Where G, Glomerulus; PCT, Proximal convoluted tubule; DCT, Distal convoluted tubule; Cr, crystal; In, Inflammation; R, Regenerative cells. Scale bar = 100 µm. Data is presented as mean ± S.E.M (n = 7 animals per group) and was analyzed by one-way ANOVA followed by Dunnett's multi-comparison test. ## $p < 0.01$ *vs.* NC; * $p < 0.05$; ** $p < 0.01$ *vs.* DC.

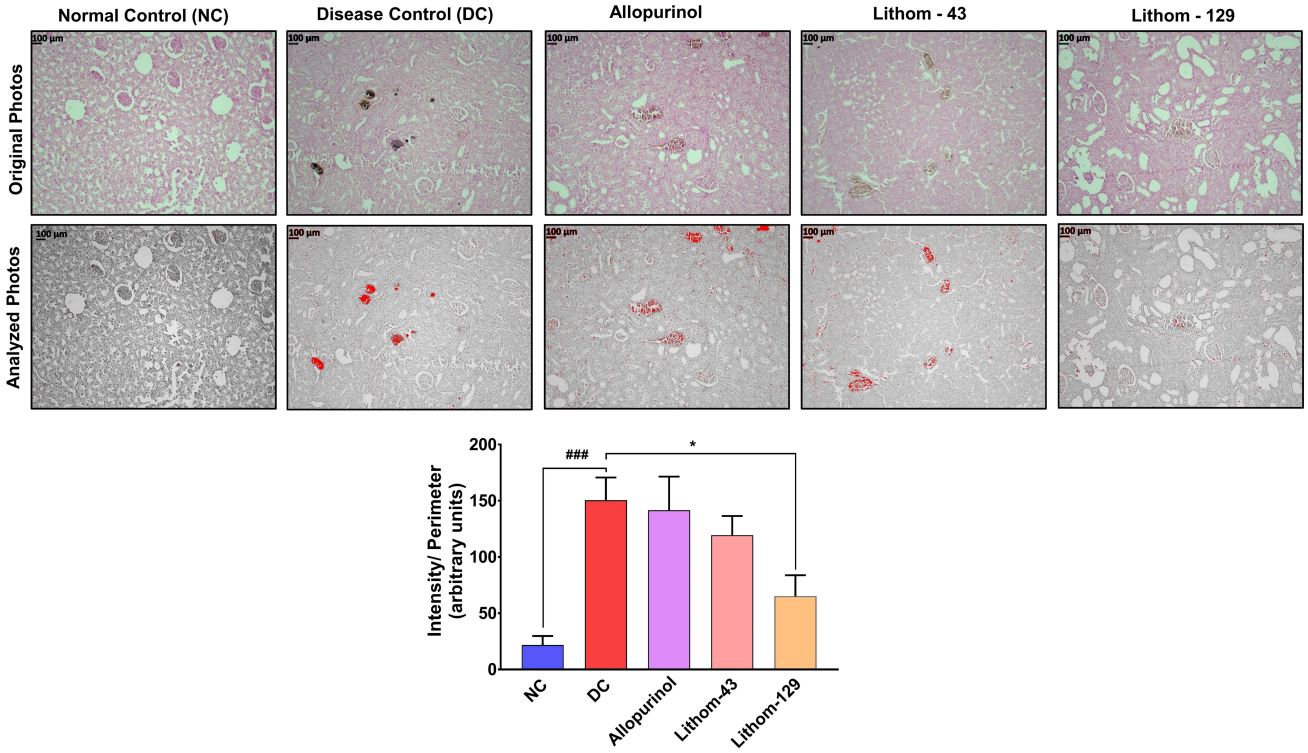

Fig. 9. Von Kossa staining of oxalate crystals in kidney sections. Representative images of von kossa stained crystals that appeared black (as shown in original photos) and their analysis using Fiji appeared red (as shown in analyzed photos) (Magnification ×100). Quantitative analysis of the intensity/perimeter ratio of the von kossa stained crystal represents a decreasing trend with increasing doses of Lithom (Lower panel). Data is presented as mean ± S.E.M (n = 7 animals per group) and was analyzed by one-way ANOVA followed by Dunnett's multi-comparison test. ### $p < 0.001$ *vs.* NC; * $p < 0.05$ *vs.* DC. Scale bar = 100 µm.

position, which was seen significantly reduced in both the Lithom-tested groups in a dose-related manner. For quantification of the stained crystals, their intensity/perimeter ratio has been estimated (Fig. 9 Lower panel) and found to be significantly ($p < 0.05$) decreased at 129 mg/kg dose of Lithom, proving the potency of Lithom in preventing the crystal-cell interactions and thereby their depositions.

Discussion

The present study aimed to evaluate the anti-urolithiatic properties of Lithom. Two of the major concerns while treating nephrolithiasis are the expulsion of the crystals from the kidney and the prevention of their recurrence. The expulsion of crystals can be done by reducing the size and altering the morphology and shape of crystals. Therefore, initially, we explored whether Lithom could affect the size and/or shape of COM crystals during their formation. Lithom displayed a significant inhibitory effect on crystals formed in its presence and more interestingly this effect was clearly dose-dependent. The presence of Lithom during crystal formation not only regularized the shape of COM crystals but also smoothened their edges and reduced their overall sizes. Alteration of sharp polygonal crystals into regular and spherical shapes signifies the transition of COM into COD which is less harmful. These spherical-shaped crystals provide lesser surface area for crystal-cell interaction and its attachment with renal epithelium, implying their improved expulsion from the kidney due to the diuretic effect of Lithom. Moreover, the surface topography of crystals from irregular, sharp-edged polygons is altered to smooth, regular, uniform flattened cuboids due to Lithom treatment. This change makes Lithom-treated crystals more amenable to the hydrodynamic effects of urine flow facilitating their easy expulsion. Hence, Lithom hampers the process of COM crystallization as observed from the decrease in area and Feret diameter of the COM crystals. Similar findings were observed in our *in vivo* study where it was found that the presence of oxalate crystals in urine drastically decreased in the Lithom-treated groups which signifies that Lithom might be reducing crystalluria by inhibition of the supersaturation step. This property of Lithom might be due to the presence of Bergenin as one of its phytoconstituents. Bergenin is a c-glucoside of o-methyl gallic acid, majorly present in the species of Bergenia [39]. In the Ayurvedic system of medicines, this plant is also known as '*pashanbheda*' (stone-breaker). Anti-urolithiasis activity can be achieved either by inhibition of oxalate aggregation or by increasing diuresis. The anti-urolithiatic efficacy of Bergenia in EG-induced hyperoxaluric rat models

has been previously reported by Sharma *et al* [24]. They have demonstrated the inhibitory effect of Bergenia against aggregation of oxalate crystals, *in vitro* [24]. A study by Chhatre *et al*. [40] has reported the anti-urolithiatic activity of *Tribulus terrestris* in a rat model of nephrolithiasis. The diuretic activity possessed by this plant is due to the presence of high concentrations of nitrates and potassium present in its fruit [40]. The extract of *Tribulus terrestris* also displayed an inhibitory effect against the crystallization and aggregation of COM, *in vitro*. As *Tribulus terrestris* is a major component of Lithom, the observed normalization of urinary oxalate and citrate levels upon treatment with Lithom in EG-induced rats might be due to the effects of its phytocomponents. Aggarwal *et al*. [41] have shown that protein isolated from *Tribulus terrestris* showed similarities with carotenoid cleavage dioxygenase 7 (CCD7) and demonstrated a cryoprotective action on oxalate-induced NRK-52E cells.

Oxidative stress arises due to an imbalance between the reactive oxygen species and endogenous antioxidant levels [42–44]. Several herbal formulations are known to possess anti-oxidant activity [45,46]. Hyperoxaluria-induced renal injury occurs primarily through lipid peroxidation [47]. Abrasive interactions between oxalate crystals and renal epithelial cells damage the membranes releasing intracellular contents, that serve as focal points for crystal aggregation [48,49]. Malondialdehyde (MDA) is the basal product of lipid peroxidation, an increase in MDA level signifies a high rate of lipid peroxidation in tissue [50,51]. Hence amelioration of MDA level through Lithom treatment could be an effective method to focus on. Catalase is the key antioxidant enzyme that is responsible for the decomposition of hydrogen peroxide (H_2O_2) into water and oxygen, its deficiency would increase the level of H_2O_2 in tissue, which brings an imbalance in the antioxidant system rendering the tissue susceptible to injury [52,53]. In this study, a decrease in catalase activity has been observed in the disease control group, which has been restored to normal by Lithom treatment administration. Myeloperoxidase (MPO) is an antioxidant enzyme inhibited by an increased level of H_2O_2 [54]. Hence, Lithom treatment could be an efficacious way to the restoration of the hyperoxaluria-induced oxidative stress in kidneys. The proximal convoluted tubule (PCT) is the part of the nephron where maximum absorption of ions takes place, hence acting as the best site for crystal interaction and their adhesion with further injury. Histopathology of EG induced group has shown the crystal depositions in PCT with an elevation in crystal score, surrounded by the release of a massive number of inflammatory cells, depicting an elevation in total lesion score. Whereas, the Lithom treated group has shown an influx of regenerative cells in the tubular part with a significant reduction in the number of inflammatory cells, as evident from histopathology. However, further confirmation of crystal depositions in kidney sections was done by von kossa staining, which showed a dose-dependent reduction in crystal depositions. The antioxidative effect of Lithom might be due to the presence of Trigonelline, Boeravinone B, Ellagic acids, and Vanillic acids in Lithom. Trigonelline is an alkaloid present abundantly in seeds of *Trigonella foenum graecum.* Trigonelline is known to have a reducing effect on oxalate-induced intracellular ROS levels in cultured renal epithelial cells [55]. It has also shown an antioxidative effect in EG-induced oxalate rat models of nephrolithiasis [56,57]. Moreover, Trigonelline is a zwitterion, formed by methylation of nitrogen atom of Vitamin B_3. Being zwitterionic in nature, it can maintain the pH of urine, which impacts the supersaturation of oxalate in urine and prevents crystallization. It is also a known osmoregulator in plants as well as in animals, which has shown a potential effect in inhibition of solute resorption, and hence beneficial in the reduction of the recurrence rate of biomineralization in animals [23]. Boeravinone B, a retinoid isolated from roots of *Boerhavia diffusa* [9] is known to exert an antioxidant effect [58,59] in EG-induced hyperoxaluria model of nephrolithiasis by restoration of antioxidant system (MDA, Catalase, GPx, GSH, GST, SOD) [37]. Vanillic acid is a polyphenolic compound with known anti-urolithiatic properties through its inhibitory effect on crystal aggregation [60], as demonstrated earlier by Torzewska *et al*. [61] in an *in vitro* study in struvite and apatite crystal aggregation assay. It also acts as a potent antioxidant and anti-inflammatory agent *in vivo* [62,63].

The anti-inflammatory effects of Lithom might have been contributed by adenosine. There are 4 types of adenosine receptors present in mammalian renal cells namely A_1, A_{2A}, A_{2B}, and A_3. A_1 adenosine receptors are widely expressed in the PCT part and are highly responsible for the maintenance of glomerular filtration rate, resorption of solutes (ions and water), maintenance of renal vascular tone, and ATP synthesis. The rate of adenosine formation in the kidney gets enhanced during increased consumption of ATP, which is a direct result of hypoxia eventually inducing injury and inflammation to the cells [64]. This injury can be ameliorated by the supplementation of adenosine agonists. This concept is also supported by Sang won park in his study where A1 adenosine receptor activation by its agonist has shown a protective effect in acute kidney injury [65]. The herbal components of Lithom have been cited in the traditional medicinal text Bhavprakash Nighantu to provide protection against nephrolithiasis. All classical Ayurvedic formulations incorporated in the formulation of Lithom are basically kshara or alkalinizing agents that can raise the pH of oxalate-rich urine and prevent the precipitation step during crystallization [66]. This might be responsible for the observed decrease in the crystal depositions in the kidney of Lithom-treated rats.

The use of Allopurinol is being done in clinical settings in patients with nephrolithiasis but its use has been linked to cutaneous reactions that have a high mortality rate

[67]. Hence, the use of Lithom which is formulated from nature's apothecary is a viable alternative for the management of nephrolithiasis. The lack of clinical trial becomes one of the limitations of this study but the findings of this study suggest that Lithom considerably impacted the morphology and amount of COM crystal formation as evident from the *in vitro* data and histopathological data from the *in vivo* study. Also, in regards to the urine microscopy, urine biochemistry, oxidative stress level, the effectiveness of Lithom treatment ameliorated crystal depositions, inflammation, and injury associated with it.

Conclusion

The current study shows that the herbo-mineral formulation Lithom has depicted a significant anti-nephrolithiatic activity against the EG-induced rat model of nephrolithiasis. Based on the findings, it has been observed that the Lithom intervention has an inhibitory effect on crystal synthesis *in vitro* and prevention of oxalate crystal deposition in renal tubules *in vivo*. It also has shown an amelioration in oxalate excretion, reduction in lipid peroxidation, restoration of the antioxidant enzyme activity, and repairing renal damage imposed by hyperoxaluria. Though, throughout the study, we have a clear understanding of how EG induction and Lithom intervention have impacted metabolic levels, its impact on the genetic level is yet to be discovered. Further effects of Lithom on gene expression of renal tubular cells induced with COM crystals will provide a molecular pathway of the bioactivities of Lithom.

Availability of Data and Materials

All data generated or analyzed during this study are included in this article. Further enquiries can be directed to the corresponding author.

Author Contributions

AB: Conceptualization, planning, visualization, supervision, writing — review & editing. SS: Conceptualization, planning, visualization, methodology, investigation, data curation, formal analysis, writing original draft. MMan: Methodology, investigation, formal analysis, writing original draft. AP: Methodology, investigation, formal analysis, writing original draft. MMai: Methodology, investigation, formal analysis, data curation, writing original draft. RD: Data curation, writing original draft, writing — review & editing, visualization, project administration, supervision. AV: Writing — review & editing, project administration, conceptualization, visualization, supervision. All authors contributed to the article and approved the submitted version. All authors have participated in the work and agreed to be accountable for all aspects of the work.

Ethics Approval and Consent to Participate

The animal experimental procedures were duly approved by the Institutional Animal Ethics Committee of Patanjali Research Foundation, Haridwar (vide protocol # PRIAS/LAF/IAEC-082).

Acknowledgment

The research work was funded internally by Patanjali Research Foundation Trust, Haridwar, India. The authors are thankful to Ms. Meenu Tomer, Mr. Sudeep Verma and Dr. Jyotish Srivastava for phytochemical analysis support. Authors are thankful to Mr. Shadrak Karumuri, Ms. Deepika Kumari, Ms. Deepika Mehra, and Mr. Ramhari Sharma for *in vivo* biology support. We extend our gratitude to Dr. Swati Haldar for her help in data analysis; Dr. Niti Sharma for her support in measuring oxidative stress parameters; Dr. Devika Balagopalan and Dr. Vivek Gohel for their comments on the manuscript. We are also grateful to Mr. Tarun Rajput and Mr. Gagan Kumar for their swift administrative supports.

Funding

This research received no external funding.

Conflict of Interest

The test formulation (Lithom) was provided by Divya Pharmacy, Haridwar, Uttarakhand, India. Lithom is a marketed medicinal product of Divya Pharmacy, Haridwar, India. Acharya Balkrishna is an honorary trustee in Divya Yog Mandir Trust, which governs Divya Pharmacy, Haridwar. In addition, he holds an honorary managerial position in Patanjali Ayurved Ltd, Haridwar, India. Divya Pharmacy, Haridwar and Patanjali Ayurved Ltd. Haridwar manufacture and sell many herbal medicinal products. Other than providing the test formulation (Lithom), Divya Pharmacy was not involved in any aspect of the research reported in this study. All other authors have declared no competing interests.

References

[1] Shastri S, Patel J, Sambandam KK, Lederer ED. Kidney Stone Pathophysiology, Evaluation and Management: Core Curriculum 2023. American Journal of Kidney Diseases: the Official Journal of the National Kidney Foundation. 2023; 82: 617–634.

[2] Alexander RT, Fuster DG, Dimke H. Mechanisms Underlying Calcium Nephrolithiasis. Annual Review of Physiology. 2022; 84: 559–583.

[3] Cicerello E, Mangano MS, Cova G, Ciaccia M. Changing in gender prevalence of nephrolithiasis. Urologia. 2021; 88: 90–93.

[4] Bishop K, Momah T, Ricks J. Nephrolithiasis. Primary Care. 2020; 47: 661–671.

[5] Geraghty R, Wood K, Sayer JA. Calcium oxalate crystal depo-

sition in the kidney: identification, causes and consequences. Urolithiasis. 2020; 48: 377–384.
[6] Han H, Segal AM, Seifter JL, Dwyer JT. Nutritional Management of Kidney Stones (Nephrolithiasis). Clinical Nutrition Research. 2015; 4: 137–152.
[7] Ratkalkar VN, Kleinman JG. Mechanisms of Stone Formation. Clinical Reviews in Bone and Mineral Metabolism. 2011; 9: 187–197.
[8] Sheng X, Ward MD, Wesson JA. Crystal surface adhesion explains the pathological activity of calcium oxalate hydrates in kidney stone formation. Journal of the American Society of Nephrology: JASN. 2005; 16: 1904–1908.
[9] Manzoor MAP, Agrawal AK, Singh B, Mujeeburahiman M, Rekha PD. Morphological characteristics and microstructure of kidney stones using synchrotron radiation μCT reveal the mechanism of crystal growth and aggregation in mixed stones. PLoS ONE. 2019; 14: e0214003.
[10] Ang AJS, Sharma AA, Sharma A. Nephrolithiasis: Approach to Diagnosis and Management. Indian Journal of Pediatrics. 2020; 87: 716–725.
[11] Lin BB, Lin ME, Huang RH, Hong YK, Lin BL, He XJ. Dietary and lifestyle factors for primary prevention of nephrolithiasis: a systematic review and meta-analysis. BMC Nephrology. 2020; 21: 267.
[12] Mykoniatis I, Pyrgidis N, Tzelves L, Pietropaolo A, Juliebø-Jones P, De Coninck V, *et al*. Assessment of single-probe dual-energy lithotripters in percutaneous nephrolithotomy: a systematic review and meta-analysis of preclinical and clinical studies. World Journal of Urology. 2023; 41: 551–565.
[13] Srisubat A, Potisat S, Lojanapiwat B, Setthawong V, Laopaiboon M. Extracorporeal shock wave lithotripsy (ESWL) versus percutaneous nephrolithotomy (PCNL) or retrograde intrarenal surgery (RIRS) for kidney stones. The Cochrane Database of Systematic Reviews. 2014; CD007044.
[14] Alexander RT, McArthur E, Jandoc R, Welk B, Fuster DG, Garg AX, *et al*. Thiazide Diuretic Dose and Risk of Kidney Stones in Older Adults: A Retrospective Cohort Study. Canadian Journal of Kidney Health and Disease. 2018; 5: 2054358118787480.
[15] Chung KJ, Kim JH, Min GE, Park HK, Li S, Del Giudice F, *et al*. Changing Trends in the Treatment of Nephrolithiasis in the Real World. Journal of Endourology. 2019; 33: 248–253.
[16] Balkrishna A, Sharma S, Gohel V, Kumari A, Rawat M, Maity M, *et al*. Renogrit attenuates Vancomycin-induced nephrotoxicity in human renal spheroids and in Sprague-Dawley rats by regulating kidney injury biomarkers and creatinine/urea clearance. PLoS ONE. 2023; 18: e0293605.
[17] Balkrishna A, Gohel V, Pathak N, Bhattacharya K, Dev R, Varshney A. Livogrit prevents Amiodarone-induced toxicity in experimental model of human liver (HepG2) cells and *Caenorhabditis elegans* by regulating redox homeostasis. Drug and Chemical Toxicology. 2024; 1–17.
[18] Dhiman S, Srikant N, Pant P, Singh R, Sharma H, Singh A. Identification and Quantification of Boeravinone-B in dry fruit extract of Boerhaavia diffusa Linn and in its Polyherbal Formulation. Journal of Natural Remedies. 2017; 17: 1–8.
[19] Pandey MM, Rastogi S, Rawat AK. Indian traditional ayurvedic system of medicine and nutritional supplementation. Evidence-based Complementary and Alternative Medicine: ECAM. 2013; 2013: 376327.
[20] Al-Mamoori FF. Natural products for the prevention and management of nephrolithiasis. In Meena SN, Nandre V, Kodam K, Meena RS (eds.) New Horizons in Natural Compound Research (pp. 225–230). Academic Press: MA. 2023.
[21] Kaushik S, Choudhary M, Rajpal S. Antiurolithiatic efficacy of combination preparations of Dolichos biflorus and Crataeva nurvala: folk medicines used in Indian traditional medicine. Future Journal of Pharmaceutical Sciences. 2021; 7: 21.
[22] Aggarwal A, Tandon S, Singla SK, Tandon C. Diminution of oxalate induced renal tubular epithelial cell injury and inhibition of calcium oxalate crystallization in vitro by aqueous extract of Tribulus terrestris. International Braz J Urol: Official Journal of the Brazilian Society of Urology. 2010; 36: 480–488; discussion 488, 489.
[23] Kapase C, Bodhankar S, Mohan V, Thakurdesai P. Therapeutic effects of standardized fenugreek seed extract on experimental urolithiasis in rats. Journal of Applied Pharmaceutical Science. 2013; 3: 29–35.
[24] Sharma I, Khan W, Parveen R, Alam MJ, Ahmad I, Ansari MH, *et al*. Antiurolithiasis Activity of Bioactivity Guided Fraction of *Bergenia ligulata* against Ethylene Glycol Induced Renal Calculi in Rat. BioMed Research International. 2017; 2017: 1969525.
[25] Pantha R, Pandey J, Joshi N, Budathoki R, Ghimire S, Pokhrel T, *et al*. Anti-urolithiatic Property of Crataeva nurvala Root and Bark from Nepal on Ethylene Glycol induced Urolithiatic Mice. Journal of Pharmaceutical Sciences and Research. 2020; 12: 658–662.
[26] Kant R, Singh TG, Singh S. Mechanistic approach to herbal formulations used for urolithiasis treatment. Obesity Medicine. 2020; 19: 100266.
[27] Chaiyarit S, Thongboonkerd V. Defining and Systematic Analyses of Aggregation Indices to Evaluate Degree of Calcium Oxalate Crystal Aggregation. Frontiers in Chemistry. 2017; 5: 113.
[28] Nair AB, Jacob S. A simple practice guide for dose conversion between animals and human. Journal of Basic and Clinical Pharmacy. 2016; 7: 27–31.
[29] Ozturk H, Cetinkaya A, Firat TS, Tekce BK, Duzcu SE, Ozturk H. Protective effect of pentoxifylline on oxidative renal cell injury associated with renal crystal formation in a hyperoxaluric rat model. Urolithiasis. 2019; 47: 415–424.
[30] Sener TE, Sener G, Cevik O, Eker P, Cetinel S, Traxer O, *et al*. The Effects of Melatonin on Ethylene Glycol-induced Nephrolithiasis: Role on Osteopontin mRNA Gene Expression. Urology. 2017; 99: 287.e9–287.e15.
[31] Millan A, Conte A, Garcia-Raso A, Grases F. Determination of citrate in urine by simple direct photometry. Clinical Chemistry. 1987; 33: 1259–1260.
[32] Bergerman J, Elliot JS. Method for Direct Colorimetric Determination of Oxalic Acid. Analytical Chemistry. 2002; 27: 1014–1015.
[33] Benhelima A, Kaid-Omar Z, Hemida H, Benmahdi T, Addou A. Nephroprotective and diuretic effect of Nigella sativa L seeds oil on lithiasic wistar rats. African Journal of Traditional, Complementary, and Alternative Medicines. 2016; 13: 204–214.
[34] Goth L. A simple method for determination of serum catalase activity and revision of reference range. Clinica Chimica Acta; International Journal of Clinical Chemistry. 1991; 196: 143–151.
[35] Heath RL, Packer L. Photoperoxidation in isolated chloroplasts. I. Kinetics and stoichiometry of fatty acid peroxidation. Archives of Biochemistry and Biophysics. 1968; 125: 189–198.
[36] Kettle AJ, Gedye CA, Hampton MB, Winterbourn CC. Inhibition of myeloperoxidase by benzoic acid hydrazides. The Biochemical Journal. 1995; 308 (Pt 2): 559–563.
[37] Yang X, Ding H, Qin Z, Zhang C, Qi S, Zhang H, *et al*. Metformin Prevents Renal Stone Formation through an Antioxidant Mechanism In Vitro and In Vivo. Oxidative Medicine and Cellular Longevity. 2016; 2016: 4156075.
[38] Pareta SK, Patra KC, Mazumder PM, Sasmal D. Aqueous extract of Boerhaavia diffusa root ameliorates ethylene glycol-induced hyperoxaluric oxidative stress and renal injury in rat kidney. Pharmaceutical Biology. 2011; 49: 1224–1233.

[39] Koul B, Kumar A, Yadav D, Jin JO. *Bergenia* Genus: Traditional Uses, Phytochemistry and Pharmacology. Molecules (Basel, Switzerland). 2020; 25: 5555.
[40] Chhatre S, Nesari T, Somani G, Kanchan D, Sathaye S. Phytopharmacological overview of Tribulus terrestris. Pharmacognosy Reviews. 2014; 8: 45–51.
[41] Aggarwal A, Tandon S, Singla SK, Tandon C. A novel antilithiatic protein from Tribulus terrestris having cytoprotective potency. Protein and Peptide Letters. 2012; 19: 812–819.
[42] Wang Y, Jiang H, Zhang L, Yao P, Wang S, Yang Q. Nanosystems for oxidative stress regulation in the anti-inflammatory therapy of acute kidney injury. Frontiers in Bioengineering and Biotechnology. 2023; 11: 1120148.
[43] Su S, Ma Z, Wu H, Xu Z, Yi H. Oxidative stress as a culprit in diabetic kidney disease. Life Sciences. 2023; 322: 121661.
[44] Srivastava A, Tomar B, Sharma D, Rath SK. Mitochondrial dysfunction and oxidative stress: Role in chronic kidney disease. Life Sciences. 2023; 319: 121432.
[45] Balkrishna A, Gohel V, Pathak N, Singh R, Tomer M, Rawat M, *et al*. Anti-oxidant response of lipidom modulates lipid metabolism in Caenorhabditis elegans and in OxLDL-induced human macrophages by tuning inflammatory mediators. Biomedicine & Pharmacotherapy = Biomedecine & Pharmacotherapie. 2023; 160: 114309.
[46] Balkrishna A, Gohel V, Pathak N, Tomer M, Rawat M, Dev R, *et al*. Anti-hyperglycemic contours of Madhugrit are robustly translated in the *Caenorhabditis elegans* model of lipid accumulation by regulating oxidative stress and inflammatory response. Frontiers in Endocrinology. 2022; 13: 1064532.
[47] Tungsanga K, Sriboonlue P, Futrakul P, Yachantha C, Tosukhowong P. Renal tubular cell damage and oxidative stress in renal stone patients and the effect of potassium citrate treatment. Urological Research. 2005; 33: 65–69.
[48] Selvam R. Calcium oxalate stone disease: role of lipid peroxidation and antioxidants. Urological Research. 2002; 30: 35–47.
[49] Wigner P, Grębowski R, Bijak M, Szemraj J, Saluk-Bijak J. The Molecular Aspect of Nephrolithiasis Development. Cells. 2021; 10: 1926.
[50] Pradini A, Anggraeny D, Bisri T, Akmalia D. Effect of antioxidants on kidney damage repair in-diabetes-induced animal: a literature study. ACTA Medical Health Sciences. 2023; 2: 46–53.
[51] Baltusnikiene A, Staneviciene I, Jansen E. Beneficial and adverse effects of vitamin E on the kidney. Frontiers in Physiology. 2023; 14: 1145216.
[52] Emami E, Talebi-Boroujeni P, Sherwin CM, Heidari-Soureshjani S, Mohammadi S. Effect of Curcumin on Oxidative Stress, Inflammatory Response and Kidney Biochemical Parameters Among Kidney Disease Patients: A Systematic Review. The Natural Products Journal. 2023; 13: 86–97.
[53] Su L, Zhang J, Gomez H, Kellum JA, Peng Z. Mitochondria ROS and mitophagy in acute kidney injury. Autophagy. 2023; 19: 401–414.
[54] Davies MJ. Myeloperoxidase-derived oxidation: mechanisms of biological damage and its prevention. Journal of Clinical Biochemistry and Nutrition. 2011; 48: 8–19.
[55] Peerapen P, Thongboonkerd V. Protective roles of trigonelline against oxalate-induced epithelial-to-mesenchymal transition in renal tubular epithelial cells: An in vitro study. Food and Chemical Toxicology: an International Journal Published for the British Industrial Biological Research Association. 2020; 135: 110915.
[56] Shekha MS, Qadir AB, Ali HH, Selim XE. Effect of Fenugreek (Trigonella Foenum-Graecum) on Ethylene Glycol Induced Kidney Stone in Rats. Jordan Journal of Biological Sciences. 2014; 7: 257–260.
[57] Laroubi A, Touhami M, Farouk L, Zrara I, Aboufatima R, Benharref A, *et al*. Prophylaxis effect of Trigonella foenum graecum L. seeds on renal stone formation in rats. Phytotherapy Research: PTR. 2007; 21: 921–925.
[58] Muley MM, Doshi SM, Goyal A, Jachak SM. Ethnopharmacology and Phytochemistry of Selected Species of Boerhavia Occurring in India: A Review. Current Traditional Medicine. 2023; 9: 93–113.
[59] Santhosh S, Pazhani G, Arathi M, Manickam S. Nephroprotective Role of Boerhavia diffusa in Renal Disorders: A Review. Research Journal of Pharmacy. 2023; 16: 962–968.
[60] Hefer M, Huskic IM, Petrovic A, Raguz-Lucic N, Kizivat T, Gjoni D, *et al*. A Mechanistic Insight into Beneficial Effects of Polyphenols in the Prevention and Treatment of Nephrolithiasis: Evidence from Recent In Vitro Studies. Crystals. 2023; 13: 1070.
[61] Torzewska A, Rozalski A. Inhibition of crystallization caused by Proteus mirabilis during the development of infectious urolithiasis by various phenolic substances. Microbiological Research. 2014; 169: 579–584.
[62] Ahmed S, Hasan MM, Khan H, Mahmood ZA, Patel S. The mechanistic insight of polyphenols in calcium oxalate urolithiasis mitigation. Biomedicine & Pharmacotherapy = Biomedecine & Pharmacotherapie. 2018; 106: 1292–1299.
[63] Sindhu G, Nishanthi E, Sharmila R. Nephroprotective effect of vanillic acid against cisplatin induced nephrotoxicity in wistar rats: a biochemical and molecular study. Environmental Toxicology and Pharmacology. 2015; 39: 392–404.
[64] Yap SC, Lee HT. Adenosine and protection from acute kidney injury. Current Opinion in Nephrology and Hypertension. 2012; 21: 24–32.
[65] Park SW, Chen SW, Kim M, Brown KM, D'Agati VD, Lee HT. Protection against acute kidney injury via A(1) adenosine receptor-mediated Akt activation reduces liver injury after liver ischemia and reperfusion in mice. The Journal of Pharmacology and Experimental Therapeutics. 2010; 333: 736–747.
[66] Bhende S, Parwe S. Ayurveda management of Mutrashmari with special respect to urolithiasis: A case study. Journal of Indian System of Medicine. 2019; 7: 189–193.
[67] Stamp LK, Chapman PT. Allopurinol hypersensitivity: Pathogenesis and prevention. Best Practice & Research. Clinical Rheumatology. 2020; 34: 101501.